

The Potential Barrier Heights and the Carrier Densities of ZnO Varistors with Various Compositions

Sung Gurl Cho, Min Hwan Kwak, Sang Ki Lee and Hyung Sik Kim*

Department of Electronic Materials Engineering and Advanced Materials Research Institute,
Gyeongsang National University, Chinju, Gyeongnam 660-701, Korea

*Korea Electrotechnology Research Institute, Changwon, Gyeongnam 641-120, Korea

(Received February 27, 1998)

The barrier heights and carrier densities of ZnO varistors with various compositions were estimated using C-V, J-V and ρ -T relations. The barrier heights obtained from C-V and J-V plots were 0.73-5.98 eV and 0.25-2.70 eV, respectively. The carrier densities estimated from C-V plots were $\sim 10^{18}$ cm⁻³. Acceptable values of the barrier heights and the carrier densities were obtained from ρ -1/T curves and the capacitances at zero bias; 0.6-0.8 eV for the barrier heights and $\sim 10^{17}$ cm⁻³ for carrier densities. Addition of cobalt increased the barrier height and the carrier density, while chromium slightly lowered both of them.

Key words : ZnO varistor, Barrier height, Carrier density, Cobalt oxide, Chromium oxide

I. Introduction

Highly nonlinear current-voltage characteristics of ZnO varistors are generally explained using Schottky barriers at the grain boundaries.¹⁾ The potential barriers and donor concentrations (or electron densities) have been estimated using current-voltage relations^{2,3)} and capacitance-voltage relations^{4,5)} developed for metal-semiconductor or metal-insulator-semiconductor junctions. Morris⁶⁾ first calculated the potential barrier height at the ZnO varistor grain boundaries and donor density in the grains applying capacitance-voltage relation developed for metal-semiconductor junction. The barrier height of 1.75 eV and donor density, $N_d = 1.2 \times 10^{19}$ cm⁻³, were obtained. However, the barrier height, 1.75 eV, is much larger than those obtained from the dependence of Schottky emission current on temperature, 0.53-0.81 eV.^{4,6)} Mukae *et al.*⁵⁾ suggested a modified C-V relation accounting forward-biased, other side of a back-to-back Schottky barriers, which is

$$\left(\frac{1}{C} - \frac{1}{2C_0}\right)^2 = \frac{2}{q\epsilon N_d} (\Phi_b + V) \quad (1)$$

$$\frac{1}{C_0} = 2 \left(\frac{2\Phi_b}{q\epsilon N_d}\right)^{1/2} \quad (2)$$

where C is the capacitance per unit grain boundary area, C_0 is the capacitance at $V=0$, q is the electron charge, ϵ is the permittivity of ZnO ($8.5\epsilon_0$), N_d is the donor density of ZnO grain, Φ_b is the built-in potential, and V is the applied voltage. Regarding the above equations it should be pointed out that in the C-V relation developed in metal-semiconductor junction Φ_b is not the barrier height but the built-in potential.⁷⁾ Therefore energy difference

between the conduction band edge and the Fermi level should be added to Φ_b for obtaining a correct barrier height Φ . Also a donor density, N_d , is not appropriate to adopt for ZnO varistor. Since it is assumed in the equation that the donors in semiconductors are mostly ionized at room temperature, the concentration of ionized donors, N_d^+ , which is the parameter included in determining the depletion width, is same as N_d . For ZnO varistors, however, various donors having different energy distances from conduction band edge are present.^{1,8)} Therefore it seems more adequate to use the carrier density, n, rather than the donor density, N_d . Nevertheless the advantage of using C-V relation is that both barrier height and carrier density can be calculated simultaneously

When thermionic emission is the major conduction mechanism, the current density for metal-semiconductor junction can be expressed as,⁷⁾

$$J = A^* T^2 \exp\left(-\frac{q\Phi}{kT}\right) \exp\left(\frac{qV}{kT}\right) \quad (3)$$

where A^* is effective Richardson constant, Φ is the potential barrier height, k is the Boltzmann constant, and T is the absolute temperature. Assuming Schottky (Poole-Frenkel) emission as major conduction process, then current-voltage relation can be expressed as,^{2,9)}

$$J \propto \exp\left(-\frac{q\Phi}{kT}\right) \exp\left(\frac{\beta V^{1/2}}{kT}\right) \quad (4)$$

where β is the Schottky field-lowering coefficient. We used voltage per grain boundary, V, instead of electric field shown in references, because determination of electric field at junction is hard to achieve.

The barrier height has been obtained using a resistivity-temperature relation in the low current level (prebreakdown region) expressed as follows,^{10,11)}

$$\rho = \rho_0 \exp(q\Phi/kT) \quad (5)$$

where ρ is the resistivity of the specimen, ρ_0 is a constant.

In this study barrier heights and carrier densities of ZnO varistors containing basic additives such as bismuth, antimony, cobalt and/or chromium oxides were estimated using the capacitance-voltage relation, the current-voltage relations and the resistivity-temperature relation. The values obtained using different relations were compared and the effect of cobalt and chromium oxides were investigated.

II. Experimental Procedure

Conventional mixed oxide ceramic processing was used to prepare specimens. The chemical compositions of the specimens expressed as ZBS, ZBSCo, ZBSCr and ZBSCCr are given in Table 1. Reagent grade ZnO, Bi₂O₃, Sb₂O₃, Co₃O₄ and/or Cr₂O₃ were mixed using a ball mill with methanol and zirconia balls. The powder was granulated by passing through a sieve after mixing with PVA solution using an alumina mortar and pestle. Disc shaped green compacts with diameter of 15 mm were uniaxially pressed and sintered at 1100°C for one hour in an ambient atmosphere. The sintered specimens were cooled in the furnace which was shut off after completion of the soak time. A commercial varistor (Matsushita ZNR) was investigated for reference.

Apparent densities of all sintered specimens were measured to check the degree of densification. The fracture surfaces of the specimens were polished and chemically etched with 0.5% HF aqueous solution to examine microstructure using an optical microscope (EPIPHOTO-TME, NICON, Tokyo, Japan). Crystalline phases of the sintered specimens were analyzed using X-ray diffractometer (D/MAX-3C, Rigaku, Tokyo, Japan). Average grain sizes of the specimens were obtained using the equation proposed by Mendelson,¹²⁾ after measuring the number of grain boundary intersections per unit line length of test lines, \bar{L} , from optical micrographs.

$$\bar{D} = 1.56 \bar{L} \quad (6)$$

Table 1. Chemical Compositions of the ZnO Varistor Specimens (mol%).

Notation	Composition				
	Cr ₂ O ₃	ZnO	Bi ₂ O ₃	Sb ₂ O ₃	Co ₃ O ₄
ZBS	98%	1.0%	1.0%		
ZBSCo	98.3%	1.0%	0.5%	0.2%	
ZBSCr	98%	1.0%	0.5%		0.5%
ZBSCCr	97.5%	1.0%	0.3%	0.5%	0.7%

For electrical contact, both sides of the specimens were polished with SiC abrasive paper and cleaned ultrasonically. Aluminum electrodes were then evaporated on both sides of the samples. Current-voltage characteristics were obtained using a I-V meter (Keithley 237 High voltage source measure unit, Keithley Instruments, Cleveland, Ohio) and nonlinear coefficients were determined from the slopes in the current density range of 0.1-1.0 mA/cm².

The C-V analysis were conducted using a LF impedance analyzer (HP4192A, Hewlett Packard, Sandiego, CA) at 10 kHz and 0-40 V internal bias. The carrier concentrations and the barrier heights of the specimens were calculated from the intercepts of the C-V plots and the slopes respectively using equations (1) and (2). The current-voltage relations were measured in the temperature range of 20°-100°C for various voltage dependences. The barrier heights were estimated from $J/T^2-1/T$ curves using equations (3) and (4). The ρ -T curves were obtained using the I-V meter in the temperature range of 40°-150°C. The resistivities were calculated from the voltages measured at 1 nA and the sample geometry. The barrier heights were obtained from the slopes of the ρ -T plots using equation (5), and the carrier concentrations were estimated from the barrier heights and capacitances at zero bias, Co, using equation (2).

III. Results and discussion

Apparent densities of the specimens were in the range of 5.5-5.7 g/cm³, which are more than 97% of theoretical density of ZnO. Average grain sizes of the samples were in the range of 12-21 μ m and were given in Table 2. Typical microstructures of the specimens are shown in Fig. 1. Current-voltage relations of the ZnO varistors with different compositions are present in Fig. 2. The best varistor characteristics was obtained from ZBSCo specimens which have nonlinear coefficient of 29 and the least leakage current in the prebreakdown region. Very similar I-V curves of ZBS and ZBSCr suggest chromium alone does not improve I-V characteristic of the varistor. The current-voltage characteristics of the samples will be

Table 2. Nonlinear Coefficients, Barrier Heights and Carrier Densities of ZnO Varistors Obtained from I-V and C-V Plots

Samples	Characteristics	Carrier density (cm ⁻³)	Gram size (μ m)	Nonlinear coeff. (α)*	Barrier height (eV)
ZBS		21	7	0.73	4.6×10^{17}
ZBSCo		13	29	1.92	2.3×10^{18}
ZBSCr		15	6	5.50	2.1×10^{18}
ZBSCCr		12	12	5.98	5.9×10^{18}
ZNR		31	42	2.34	8.8×10^{17}

* Nonlinear coefficients were measured in the range of 0.1-1.0 mA/cm².

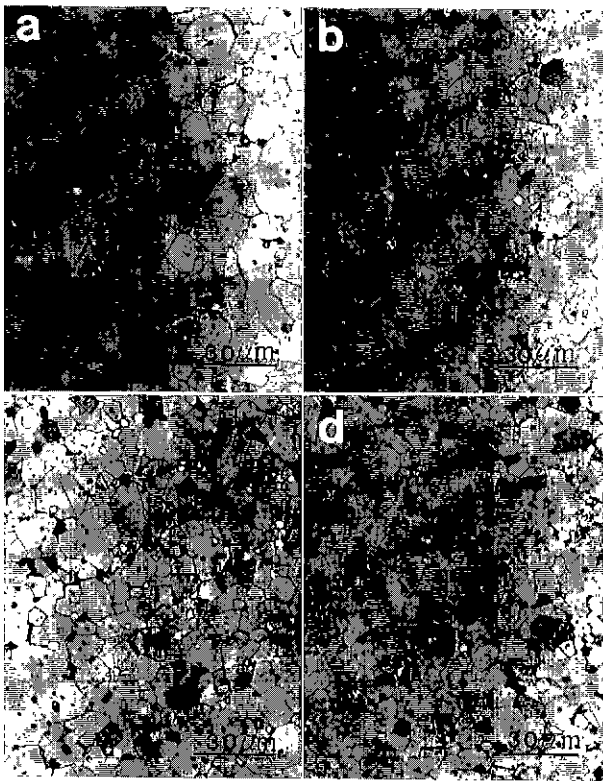


Fig. 1. Optical micrographs of ZnO varistors with various compositions sintered at 1100°C for 1 hour; (a) ZBS, (b) ZBSCr, (c) ZBSCo and (d) ZBSCCr.

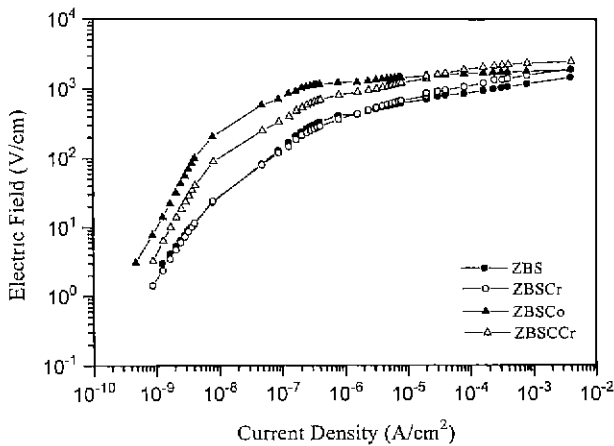


Fig. 2. I-V curves for ZnO varistors with various compositions sintered at 1100°C for 1 hour.

further discussed in conjunction with barrier heights and carrier densities.

The barrier heights, actually built-in potential, and the carrier densities for the specimens were estimated from $(1/C - 1/2C_0)^2$ vs applied bias per grain boundary plots shown in Fig. 3 and summarized in Table 2 along with the nonlinear coefficients measured in the range of 10^{-4} - 10^{-3} A/cm². The plots are out of linearity at low voltages which is often observed in the plots presented by the other researchers.^{10,13} The barrier heights determined

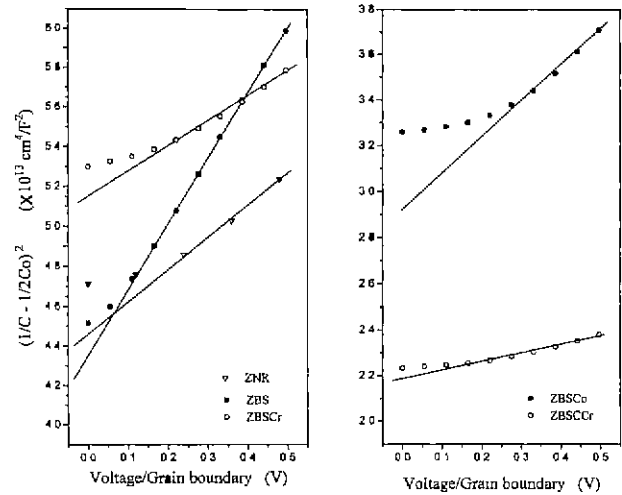


Fig. 3. C-V plots measured at 10 kHz for ZnO varistors with various compositions sintered at 1100°C for 1 hour. (A plot for commercial varistor, ZNR, is included for reference.)

from the plots are unreasonably large and in a wide range depending upon the compositions, from 0.73 eV for ZBS to 5.98 eV for ZBSCCr, which are quite different from the published data.^{2,3,10,14,16} The carrier densities, $\sim 10^{18}$ cm⁻³, are also higher than the published data by an order of magnitude.¹⁴ The barrier height and carrier density calculated for the commercial varistor also showed high value, 2.34 eV. These discrepancies are believed to be arised from the complicated grain boundaries of ZnO varistors consisting of irregular shape grain boundaries and inhomogeneous intergranular phase in comparison to the simple metal-semiconductor junctions. Even for Pb-based ZnO varistors which have much simpler grain boundaries than Bi-based ZnO varistors, the barrier heights estimated from C-V relations show diverse values from 0.83 to 1.6 eV.^{5,13,16} The barrier heights determined from C-V plots did not agree with I-V relation shown in Fig. 2. The leakage current at low voltage for ZBS and ZBSCr were almost same, but the barrier heights were 0.73 eV for ZBS and 5.50 eV for ZBSCr. It can be concluded that determination of barrier height using C-V relation is not appropriate for ZnO varistors prepared in this study.

The current-voltage relations can be expressed in various forms depending upon conduction mechanisms. A major difference, however, is barrier lowering by the applied voltage; $J \propto \exp(V)$ and $J \propto \exp(V^{1/2})$ for thermionic emission^{7,31} and $J \propto \exp(V^{1/2})$ for Schottky (Poole-Frenkel) emission.² The $\log J$ vs voltage per grain boundary (V, $V^{1/2}$, $V^{1/3}$ and $V^{1/4}$) plots measured at different temperatures were made to examine which J-V relation fits best to the experimental data. The $\log J$ vs V plot for ZBSCCr is given in Fig. 4. The linearity of other plots were very similar, therefore, it is hard to determine which barrier-lowering dependence on the bias is appropriate. The current densities at zero bias, J_0 , were estimated by the ex-

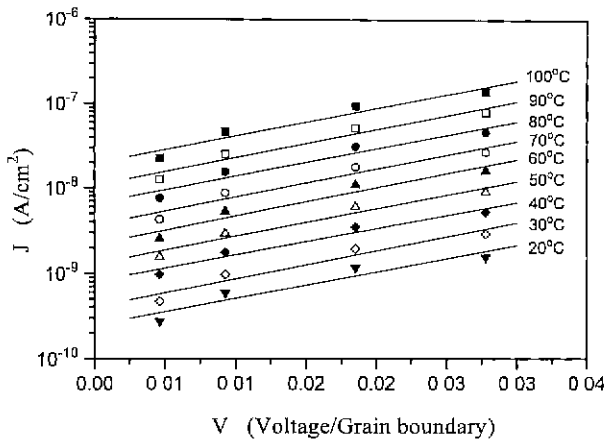


Fig. 4. J-V plots for ZBSCr specimens measured in the temperature range of 20°C-100°C. J_0 was obtained by the extrapolation of the line to $V=0$.

trapolation of the lines in Fig. 4 and used to obtain J_0/T^2 vs $1/T$ curves as shown in Fig. 5. J_0/T^2 vs $1/T$ plots for the specimens with various compositions were very different as shown in Fig. 6 for ZBSCr, so were the barrier heights evaluated from the slopes of the curves. The potential barrier heights of the specimens with various compositions were calculated for different barrier lowering by the applied voltage and summarized in Table 3. The barrier heights were in the range of 0.25-2.70 eV. When the barrier lowering by the bias is proportional to V , the smallest barrier height was 0.94 eV for ZBS and the largest one was 2.34 eV for ZBSCr. The barrier heights estimated using current-voltage relations showed similar trend with respect to the compositions of the samples as shown in Table 3, however, correlating the barrier heights to I-V relation was not successful.

The resistivities versus inverse temperatures plots show linear relation as seen in Fig. 7. The barrier heights were determined by adding 0.25 eV, which is a correction term accounting temperature dependence of the barrier height,¹⁰ to the activation energy obtained

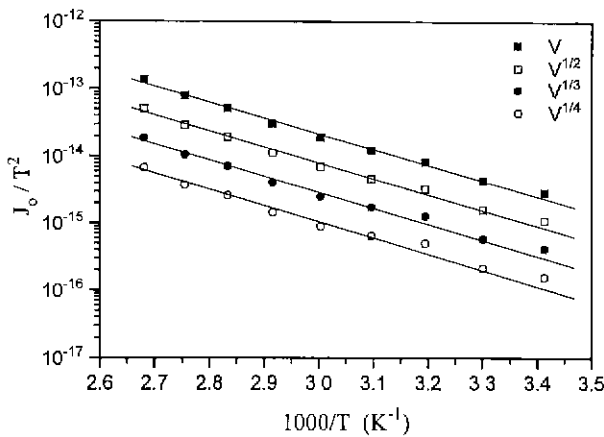


Fig. 5. J_0/T^2 vs $1/T$ curves of ZBSCr specimens for different barrier-lowering dependence on the applied voltage.

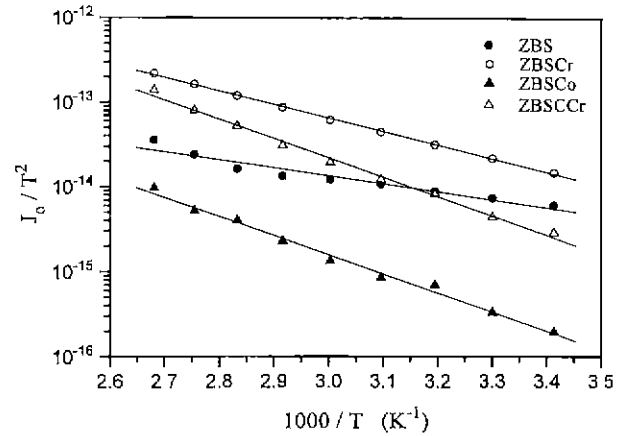


Fig. 6. J_0/T^2 vs $1/T$ curves of ZnO varistors with various compositions sintered at 1100°C for 1 hour. The plots were obtained assuming barrier-lowering is proportional to the applied voltage, V .

Table 3. Potential Barrier Heights of ZnO Varistors Estimated Using Different Barrier Lowering by the Applied Voltage. (unit: eV)

Voltage	Samples			
	ZBSCCr	ZBS	ZBSCr	ZBSCo
V	0.94	1.60	2.25	2.34
$V^{1/2}$	0.71	1.60	2.40	2.37
$V^{1/3}$	0.48	1.59	2.55	2.40
$V^{1/4}$	0.25	1.59	2.70	2.43

from the slopes of the plots. The carrier densities calculated with the barrier heights and the capacitances at zero bias determined from C-V plots shown in Fig. 3 are $\sim 10^{17} \text{ cm}^{-3}$ which agree with the published data.^{10,14} The barrier heights and carrier densities of the specimens are summarized in Table 4. The barrier heights were in the range of 0.61-0.83 eV which agree with the published data.^{1,10,15}

The effects of cobalt and chromium oxide are clearly exhibited in the data. Cobalt addition increased the barrier

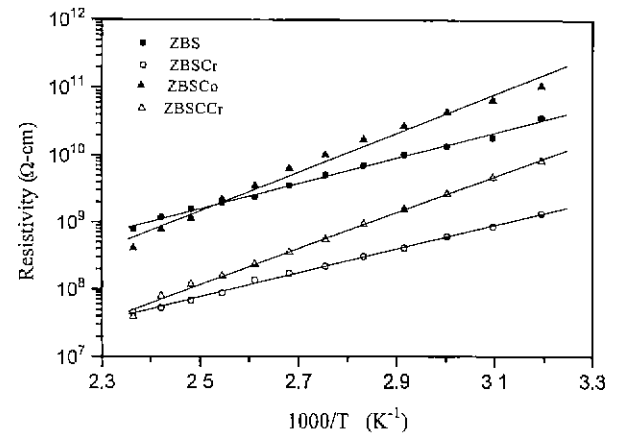


Fig. 7. ρ - T curves for ZnO varistors with various compositions sintered at 1100°C for 1 hour.

Table 4. Potential Barrier Heights and Carrier Densities of ZnO Varistors Obtained from ρ -T Plots and the Capacitances at Zero Bias.

Samples	Characteristics	Barrier height (eV)	Carrier density (cm^{-3})
ZBS		0.63	1.4×10^{17}
ZBSCo		0.83	3.9×10^{17}
ZBSCr		0.61	1.1×10^{17}
ZBSCCr		0.79	5.9×10^{17}

heights and the carrier densities, and hence the non-linear coefficients, while chromium addition slightly lowered the barrier heights and the carrier densities as shown in Table 4. The effects for the carrier densities can be understood from the facts that cobalt is distributed throughout the grains and grain boundaries, while chromium is mostly found in the grain boundaries.¹¹ Higher carrier density of ZBSCr than that of ZBSCo is attributable to their cobalt concentrations; 0.5 mol% Co_2O_3 for ZBSCr and 0.2 mol% Co_2O_3 for ZBSCo specimens.

Variation of the barrier heights and the carrier densities are well reflected in the current-voltage characteristics of the samples shown in Fig. 1. The leakage current in the prebreakdown region is low for ZBSCo, intermediate for ZBSCr and high for ZBS and ZBSCr, following the relative sizes of the barrier heights. The electric fields where breakdown of the varistors begin also agree with the barrier heights estimated; high electric field for ZBSCo, intermediate for ZBSCr and about the

same low electric fields for ZBS and ZBSCr.

The crystalline phases of the intergranular phase present in the specimens were investigated using XRD in order to find the relation with the barrier heights. XRD patterns given in Fig. 8 show suppression of pyrochlore formation by chromium addition,¹⁷⁾ however, the attempt to correlate the barrier height to the crystalline phase of the intergranular phase was not successful.

IV. Conclusion

The barrier heights and carrier densities of ZnO varistors with various compositions were estimated using C-V, J-V and ρ -T relations. The barrier heights obtained from the intercepts of $(1/C-1/2C_0)^2$ versus applied voltage per grain boundary were in the wide range with respect to the compositions of the specimens, and too high to be realistic. The carrier densities estimated from the plots were $\sim 10^{18} \text{ cm}^{-3}$, one order of magnitude larger than the published data. Although the barrier heights obtained using J-V relation showed rather reasonable values than those acquired using C-V relation, they were still too high and could not be correlated with I-V characteristics. When J-V relations were plotted with respect to V , $V^{1/2}$, $V^{1/3}$ and $V^{1/4}$, similar linearity was observed. Also J_s/T^2 vs $1/T$ plots exhibited almost the same linearity. Therefore, it should be cautious to claim the conduction mechanism by using this plot.

The barrier heights estimated from ρ - $1/T$ curves and the carrier densities obtained using the capacitances at zero bias were in the range of the published data; 0.6-0.8 eV for the barrier heights and $\sim 10^{17} \text{ cm}^{-3}$ for carrier densities. Addition of cobalt obviously increased the barrier height and the carrier density, and hence improved current-voltage characteristic. On the other hand addition of chromium slightly lowered both the barrier height and the carrier density. The effects of the additives on the barrier heights and carrier densities were well reflected in the current-voltage characteristics of the samples. It seemed not appropriate to use C-V and J-V relations developed for metal-semiconductor and MIS(metal-insulator-semiconductor) junctions to ZnO varistors with various compositions without significant modification.

References

1. T. K. Gupta, "Application of Zinc Oxide Varistors", *J. Am. Ceram. Soc.*, **73** [7] 1817-40 (1990)
2. L. M. Levinson and H. R. Philipp, "The Physics of Metal Oxide Varistors", *J. Appl. Phys.*, **46** [3] 1332-41 (1975).
3. L. K. J. Vanadamme and J. C. Brugman, "Conduction Mechanisms in ZnO Varistors", *J. Appl. Phys.*, **5** [8] 4240-44 (1980).
4. W. G. Morris, "Physical Properties of the Electrical Barriers in Varistors", *J. Vac. Sci. Technol.*, **13** [4] 926-31 (1976)
5. K. Mukae, K. Tsuda and I. Nagasawa, "Capacitance-vs-

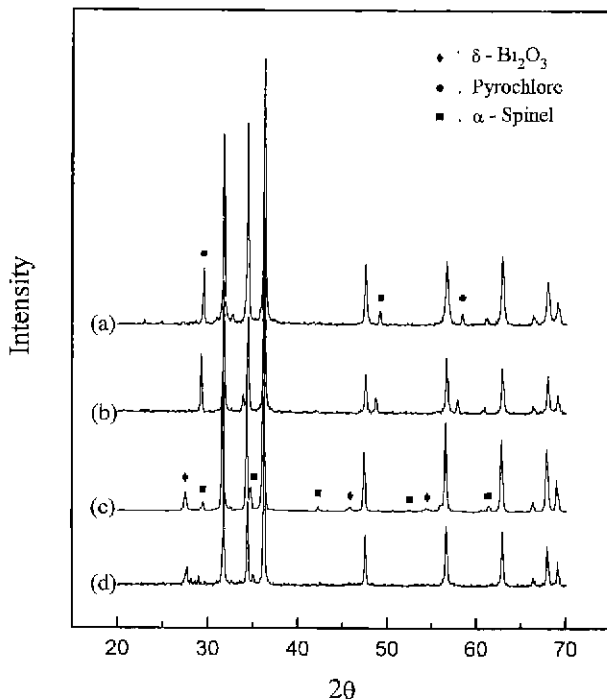


Fig. 8. XRD patterns for ZnO varistors with various compositions sintered at 1100°C for 1 hour; (a) ZBS, (b) ZBSCo, (c) ZBSCr and (d) ZBSCCr

- Voltage Characteristics of ZnO Varistors", *J. Appl. Phys.*, **50** [6] 4475-76 (1979).
6. J. D. Levine, "Theory of Varistor Electronic Properties", *Crit. Rev. Solid State Sci.*, **5** 597-608 (1975)
 7. S. M. Sze, pp. 248-288 in *Physics of Semiconductor Devices*; 2nd Ed., John Wiley & Sons, New York, 1981.
 8. J. F. Cordaro, Y. Shim and J. E. May, "Bulk Electron Traps in Zinc Oxide Varistors", *J. Appl. Phys.*, **60** [12] 4186-90 (1986).
 9. A. K. Jonscher, "Electronic Properties of Amorphous Dielectric Films", *Thin Solid Films*, **1** 213-34 (1967).
 10. T. Miyoshi, K. Maeda, K. Takahashi and T. Yamazaki, "Effect of dopants on the characteristics of ZnO varistors", pp. 309-315 in *Advances in Ceramics*, Vol. 1, *Grain Boundary Phenomena in Electronic Ceramics*, Edited by L. M. Levinson and D. C. Hill, The American Ceramic Soc., Westerville, OH, 1981.
 11. H. R. Philipp and L. M. Levinson, "High-temperature Behavior of ZnO-based Ceramic Varistors", *J. Appl. Phys.*, **50** [1] 383-89 (1979).
 12. K. L. Mendelson, "Average Grain Size in Polycrystalline Ceramics", *J. Am. Ceram. Soc.*, **52** [8] 443-46 (1969).
 13. A. B. Alles and V. L. Burdick, "The Effect of Liquid-Phase Sintering on the Properties of Pr_6O_{11} -Based ZnO Varistors", *J. Appl. Phys.*, **70** [11] 6883-90 (1991).
 14. H. R. Philipp and L. M. Levinson, "Optical Method for Determining the Grain Resistivity in ZnO-based Ceramic Varistors", *J. Appl. Phys.*, **47** [3] 1112-16 (1976).
 15. M. A. Alim, M. A. Seitz and R. W. Hirthe, "Complex Plane Analysis of Trapping Phenomena in Zinc Oxide Based Varistor Grain Boundaries", *J. Appl. Phys.*, **63** [7] 2337-45 (1988).
 16. Y.-S. Lee, K.-S. Liao and T.-Y. Tseng, "Microstructure and Crystal Phases of Praseodymium Oxides in Zinc Oxide Varistor Ceramics", *J. Am. Ceram. Soc.*, **79** [9] 2379-84 (1996).
 17. S. G. Cho, H. Lee and H. S. Kim, "Effect of Chromium on the Phase Evolution and Microstructure of ZnO doped with Bismuth and Antimony", *J. Mater. Sci.*, **32**, 4283-4287 (1997).